Aalborg Universitet

Structure and properties of Ta/Al/Ta and Ti/Al/Ti/Au multilayer metal stacks formed as ohmic contacts on n-GaN

Boturchuk, Ievgen; Walter, Thomas; Julsgaard, Brian; Khatibi, Golta; Schwarz, Sabine; Stöger-Pollach, Michael; Pedersen, Kjeld; Popok, Vladimir N.

Structure and properties of Ta/Al/Ta and Ti/Al/Ti/Au multilayer metal stacks formed as ohmic contacts on n-GaN

Ievgen Boturchuk[1], Thomas Walter[2], Brian Julsgaard[1,3], Golta Khatibi[2], Sabine Schwarz[4], Michael Stöger-Pollach[4], Kjeld Pedersen[5], Vladimir N. Popok[5,*]

Abstract

Formation of ohmic contacts to GaN is of high practical importance for device fabrication. Due to the wide band gap, formation of multilayer metal structures is required to make electrical connections with low contact resistance. The paper presents a study on structure, composition, adhesion and electrical properties of Ti/Al/Ti/Au and Ta/Al/Ta metal stacks fabricated by e-beam evaporation and thermal annealing in order to provide ohmic contacts to n-type GaN films grown on Si. For the Ti-based case, an interdiffusion of Au and Ga into the stack is found, which is probably caused by a granular structure of the top Ti layer making no proper barrier. Ti of the bottom layer is observed to diffuse into GaN, forming a thin layer of titanium nitride with a low Schottky barrier at GaN interface allowing ohmic contact as shown by electrical measurements. The Ta-based stacks have the expected layered structure with minor interdiffusion of Al and Ta at the interfaces of these two metals. No direct microscopic evidences for Ta diffusion into GaN is observed. However, the formation of a thin tantalum nitride layer at the GaN interface can be deduced from the current-voltage measurements showing ohmic electrical contacts with low contact resistivity of 1.2×10^{-3} Ohm.cm^2. Four-point bending tests on the both types of samples show that cracks always develop at the interface between Si and buffer layers of GaN. No exfoliation of the metallization layers is observed allowing us to conclude about good adhesion of the metal stacks. Thus, the fabricated Ti- and Ta-based multilayer structures show good electrical performance and reliable adhesion making them promising for the formation of ohmic contacts to n-type GaN.

* V.N. Popok
vp@mp.aau.dk

[1] Interdisciplinary Nanoscience Center (iNANO), Aarhus University, Gustav Wieds Vej 14, DK-8000 Aarhus C, Denmark

[2] Christian Doppler Laboratory Lifetime and Reliability of Interfaces in Complex Multi-Material Electronics, Technische Universität Wien, Getreidemarkt 9/164, A-1060 Wien, Austria

[3] Department of Physics and Astronomy, Aarhus University, Ny Munkegade 120, DK-8000 Aarhus C, Denmark

[4] University Service Center for Transmission Electron Microscopy, Technische Universität Wien, Wiedner Hauptstraße 8-10, 1040 Wien, Austria

[5] Department of Materials and Production, Aalborg University, Skjernvej 4A, DK-9220 Aalborg, Denmark

1 Introduction

Wide band-gap semiconductors, such as GaN and SiC, are of high interest for power electronics applications [1-3]. While fabrication of SiC-based devices has reached a considerable level of maturity, the GaN technologies still require significant development at the materials growth, device processing and packaging stages [4-6].

Growth of GaN epitaxial layers on substrates of other materials (typically, sapphire, SiC and Si) leads to high dislocation densities due to significant lattice mismatches and differences in the coefficients of thermal expansion [7-9]. On the one hand, a high defects density limits the advantages of high breakdown field strength in GaN-based power devices. On the other hand, the crystalline disorder leading to unintentional n-type doping, along with a polarization gradient at GaN/AlGaN heterointerfaces, plays an important role in the formation of a two dimensional electron gas and allows fabrication of high electron mobility transistors [10-12]. n-Type GaN is also used for Schottky diodes and metal-oxide-semiconductor field effect transistors [1]. For device fabrication, ohmic contacts are of fundamental importance to ensure appropriate operation and functioning of electronic components. In the case of an n-type semiconductor, an ohmic contact with metal can be formed if the metal work function is smaller than the semiconductor electron affinity. For GaN, publications reveal a broad range of experimentally obtained and theoretically calculated electron affinity values spanning between 2.1 and 4.2 eV [13 and references therein]. A survey of experimental results on contacts made of different metals shows that a Schottky barrier always forms on both n- and p-type GaN. Al, Ti and Cr are found to be the best candidates providing the lowest barrier for n-GaN [14]. Typically, multilayer metal stacks including Ti, Al, Ni, Cr and Ta, sometimes with a capping layer of Au, are deposited on the GaN surface using standard evaporation techniques [14-17]. These stacks require high-temperature treatment (sintering) to promote metal diffusion into the sub-surface layer of GaN in order to form conductive nitrides ensuring very low contact resistivity at the interface. Nitrogen atoms, which participate in the solid-state reactions, are withdrawn from surface region of GaN forming nitrogen vacancies therein, that enhances n-type doping at the interface. The state of the art values of contact resistivity for n-GaN are at the level of 10^{-5}-10^{-6} Ohm·cm^2 [16]. However, an important point for the formation of reliable devices is structure and adhesion of the metal contacts. This is especially a critical issue for power electronics where the thermo-mechanical stresses at interfaces due to the high temperature variations can be very large. This topic has been poorly studied so far.

Thus, formation of reliable electrical contacts to GaN is a subject of on-going research. In this paper, we

study two different metal stacks, Ta/Al/Ta and Ti/Al/Ti/Au, in order to form contacts with low resistance to n-type GaN and focus the research on structure, composition and adhesion of the metal films.

2 Experimental

2.1 Formation of metal stacks

A commercial 500 nm thick epitaxial n-type GaN film grown on a 4-inch silicon wafer (Kyma Inc.) is used for the experiments. The wafer is cleaned from possible organic contamination in water and acetone. The residuals are then removed by isopropanol. A single wafer is halved in order to form Ti-based (Ti/Al/Ti/Au, 30/90/30/60 nm) stacks on one half of the wafer and Ta-based (Ta/Al/Ta, 10/280/20 nm) on the other, thus, ensuring the same GaN quality for both cases. Thickness of the metal layers is chosen to be similar to those reported in [16, 18] for successful ohmic contact fabrication. A part of every half-wafer is used for the deposition of continuous metal layers for the mechanical and structural analysis, while on the other part the metal films are formed in ring-like shapes to perform electrical measurements (see Fig. 1).

To form the ring-shaped contacts, the samples are dehydrated on a hot plate at a temperature of 150 °C for 5 minutes and then spin-coated with the 7 % solution of polymethylmethacrylate (PMMA) in anisole. The solvent is removed by a following baking at 180 °C for 2 minutes. The contact patterns are prepared by e-beam lithography as groups of ring structures in order to enable the circular transmission line method (CTLM) for resistivity measurements (see details below). Every group of contacts consists of four structures (see insert in Fig. 1), where each structure contains a central disk of radius $r_0 = 250$ μm surrounded by 100 μm wide ring. These rings are separated from the central disk by different distances $d = 5, 10, 20$ and 40 μm. After formation of the contact patterns, the PMMA is developed using methyl isobutyl ketone-isopropanol (1:3) solution. The layer of GaN native oxide is removed by 30 seconds treatment in 5 % water solution of HCl. Then, the Ti- or Ta-based metal stacks are deposited using an e-beam evaporation system. Subsequently, the PMMA resist is lifted-off in acetone. Finally, the contacts are furnace annealed in nitrogen atmosphere for 5 minutes at 550 °C for the Ta-based structures and at 800 °C for the Ti-based ones. These temperatures have previously been shown to be optimal for obtaining low-resistivity contacts to GaN [14-16, 18].

2.2 Analysis of structure and mechanical properties

To determine the microstructure and chemical composition of the metal stacks as well as to investigate possible

diffusion occurring during heat treatment, transmission electron microscopy (TEM) and scanning TEM (STEM) investigations combined with energy dispersive X-ray (EDX) analysis and electron energy loss spectroscopy (EELS) are performed using a FEI Tecnai F20 system. TEM lamellae of the cross section of both sample types are prepared for this purpose.

To study adhesion of the metal stacks to GaN, quasi-static four-point bending (4PB) tests are carried out. The basic setup for the 4PB investigations consists of a micro tensile machine equipped with a bending module and a 500 N load cell. Using a video microscope on a software controlled xyz-stage allows in-situ monitoring of the crack opening and delamination growth during the testing. The 4PB setup has several advantages over other mixed mode testing techniques including the steady state characteristic of the crack propagation due to the constant momentum between the inner loading pins. Analytical models, based on Euler-Bernoulli beam theory are available to calculate the so-called critical energy release rate (G_c) which is an assessment of the interface toughness in dependence of the loading condition [19]. One of the problems encountered with the 4PB tests, especially in the case of brittle substrates and/or strong interfaces, is insufficient strain energy for advancement of the interface crack or occurrence of vertical cracking. To overcome these problems in this study, a symmetric sandwich sample design is realized by gluing a spring steel stiffener layer with a thickness of 700 µm on top of the metallization film stack. Prior to the testing, a notch is introduced into the Si substrate using an abrasive wire saw. During the loading, an initial crack is generated at this location and it propagates through the interface (Fig. 2). For all tests the distances between the inner loading pins and the outer supports of the 4PB jigs were 15 mm and 30 mm, respectively, with the radius of the support bearings being 1 mm. Displacement controlled loading is applied at a rate of 0.1 mm/min with load and transversal displacement monitored.

2.3 Electrical measurements

The electrical performance of ohmic contacts to semiconductors is commonly described with the area-independent parameter of specific contact resistance (or contact resistivity, ρ_c), which explicitly characterizes the resistance of the interface between the metal contact and semiconductor. In order to determine ρ_c, the current transport between lateral contacts of different geometries made to a semiconductor layer is analyzed using a transmission line model, which is a commonly accepted method since the 70s [20]. This approach can be realized by forming a sequence of rectangular pads with varying

distance between them. However, a circular contact configuration (the above mentioned CTLM) provides several advantages compared to the rectangular pads, namely, allows to simplify the contact fabrication process (by avoiding mesa structures), ensures better control in spacing between the electrodes and eliminates uncertainties due to current spreading and leakage [21]. The geometry of the contacts used in the current work is schematically shown in Fig. 3, where the total series resistance (R_S) between the ring and central disk is measured for each contact structure by a Keithley 4200-SCS semiconductor characterization system using a LakeShore probe station. The measured resistance is expected to depend on geometry and resistivities according to the formula:

$$R_S = \frac{R_{sh}}{2\pi} \left(\frac{1}{kr_0} \frac{I_0(kr_0)}{I_1(kr_0)} + \ln\left(\frac{r_1}{r_0}\right) + \frac{1}{kr_1} \frac{I_1(kr_2)K_0(kr_1) + I_0(kr_1)K_1(kr_2)}{I_1(kr_2)K_1(kr_1) - I_1(kr_1)K_1(kr_2)} \right) \approx \frac{R_{sh}}{2\pi r_0}(2L_T + d), \qquad (1)$$

where r_0, r_1, r_2 are the radii and $d = r_1 - r_0$ is the distance between the central circle and surrounding ring, as shown Fig. 3, I_n and K_n are the modified Bessel functions of first and second kind, respectively, of order n, R_{sh} is the sheet resistance, $k = \frac{1}{L_T}$ is a fitting parameter reciprocal to the transfer length $L_T = \sqrt{\frac{\rho_C}{R_{sh}}}$, which describes the length of the region below the contact where the current effectively runs in parallel in the semiconductor and in the contact. The linear approximation is valid when $L_T, d \ll r_0$. Measuring R_S for a range of geometries allows for determination of the fitting parameters and, hence, the contact resistivity.

3 Results and discussion

3.1 Characterization of structure and composition

The high-temperature treatment of the multilayered metal structures is expected to induce solid-state reactions between the metal in the bottom layer and the underlying GaN. Fig. 4 shows the schematics of this process, which is also called sintering, by an example of the Ti/Al/Ti/Au stack, where titanium nitride with low work function (ca. 4 eV) is formed at the interface with GaN [16, 22]. The surplus of this process is the generation of nitrogen vacancies in the superficial region, which are known to be an n-type dopant in GaN, thus, lowering the potential barrier for the electron transfer [15]. The capping Au layer protects the contact structure from oxidation and serves for wire bonding, while the following Ti layer should act as a barrier preventing downwards Au diffusion into the contact structure. During the sintering, Ti is also expected to form a titanium aluminide alloys with high conductance (see Fig. 4(b))

[14].

However, the structure and composition of the real sintered stacks are found to be different from the expected ones as follows from images of the Ti/Al/Ti/Au multilayer system obtained by STEM using high-angle annular dark-field (HAADF) technique (see Fig. 5). As can be seen in panel (a), the Ti and Al metal layers form granular structures, thus, making a poor barrier for Au diffusion towards the interface with GaN; this diffusion is clearly observed in Fig. 5(e). It is also found that Ga diffuses into the metal stack and intermixes with Au. Spatial maps of these two metals are found to be very similar (compare panels (b) and (e) in Fig. 5). Ga and Au practically do not mix with Al as can be seen by comparing panels (b), (c) and (e). We also do not see any strong evidences for formation of titanium aluminide alloys.

EELS spectra of the N K-edge have been recorded at the interface of the metal stack with GaN (Fig 6.). The energy loss onset at 401 eV corresponds to TiN, while the one at 405 eV to GaN. This chemical shift is caused by the difference in bonding energies of N in these two materials. Additionally, one can see that the intensity profiles vary in a different manner for GaN and TiN corresponding to the density of unoccupied states in the respective materials. These findings confirm the formation of a titanium nitride layer at the GaN/Ti interface. This thin layer can also be identified by high Ti concentration visible in the bottom of Fig. 5(d). The Ti enrichment in this layer coincides well with the strong Ga depletion seen in panel (b), thus, evidencing substitution of Ga by Ti, i.e. the TiN formation. It is worth noting that the formation of TiN layer is an important issue for ohmic contact fabrication because this material has a low electron work function enabling low contact resistance to GaN. Comparing the panels (c) and (e), one can also see that the titanium nitride layer blocks downward Au diffusion into GaN, while a very thin layer enriched by Al (panel (c)) is seen just beneath this titanium nitride suggesting presence of AlN at the interface with GaN.

Fig. 7 (a) shows much more homogeneous morphology for the case of Ta/Al/Ta stacks compared to Ti-based one. The top Ta layer and middle Al film do not contain grains. Some breakage of continuity can be seen for the Ta layer at the interface with GaN, which can be related to strong lattice mismatches as well as to Ta diffusion into GaN and tantalum nitride formation [17]. However, from the obtained TEM images we can not conclude about the latter. Fig. 7(b) and (c) indicate thin layers of Ta on both sides of the Al film as well as interdiffusion of Ta and Al at the interfaces of these two metals suggesting the formation of Ta-Al alloys. But

the middle region of Al layer is not affected by Ta diffusion. It is worth noting that our findings on structure and composition of both metallization structures correlate well with earlier literature results revealing that Ta-based stacks typically have good layered structure with smooth interfaces, while Ti-based multilayer systems show rough morphology, granulation and intermixing of components caused by annealing [18, 23].

3.2 4PB tests

Fig. 8(a) shows representative load-displacement curves obtained during the 4PB delamination tests. After a linear increase of the load, a first drop indicates the crack of the Si substrate starting at the notch growing towards the metal film stack. The following load-displacement behavior, specifically the lack of a constant load plateau is related to the elastic bending of the steel stiffener. In all samples, partial delamination at the Si/GaN interface is found, while the crack also develops inside the silicon substrate leading to brittle fracture behavior (Fig. 8 (b-c)). However, we are still able to give an estimate of G_c for the Si/GaN interface, which is found to be in the range of 11-13 J/m^2 for all samples of both types. This finding makes sense because all samples are fabricated from the same wafer, thus, we should expect stable properties. As delamination during the 4PB test always occurs along the weakest interface and no separation of the metallization layers from the GaN occurs (as can be seen in Fig. 8(c)) a good adhesion of both types of metal stacks can be concluded.

3.3 Electrical performance of ohmic contacts

Fig. 9 shows the measured resistance as a function of spacing between the central disk and surrounding rings. In order to minimize systematic uncertainties due to possible lateral differences in the quality of the ohmic contacts and/or properties of the GaN layer, each series of resistance measurements are carried out on contact structures deposited within an area of ~ 1 mm^2. Two resistance measurements for each contact separation and for each stack type (16 measurements in total) are performed. The obtained values are found to follow a linear dependence with the spacing increase (see Fig. 9) in accordance with Eq. (1). From the obtained R_s, ρ_c is found to have very close values for Ta- and Ti-based stacks, around 1.2x10^{-3} Ohm.cm^2. The fit also determines the sheet resistance $R_{sh} \approx 1.5$ kΩ/sq and the transfer length $L_T \approx 9$ μm. It is worth noting that a linear approximation requires d and $L_T \ll r_0$, which is fulfilled in our case and, thus, the parameters are consistent with the obtained linear trend.

The formed contacts of both types show fairly linear current-voltage (*IV*) characteristics indicating ohmic

nature. The most typical ones are presented in Fig. 10(a). However, for some selected structures quasi-linear *IV* curves are also found (see Fig. 10(b)), which could be caused by variations in GaN quality affecting the electron affinity value or by non-uniformity in etching of a native oxide prior to the contact fabrication. But the most probable reason would be the variation of structure and composition of the metals stacks caused by the annealing as discussed above. Inhomogeneity in diffusion processes could lead to a significant difference in electronic properties of some stacks, especially of the nitride layers at the GaN interface, thus, affecting the Schottky barrier value.

Although, the obtained values of ρ_c (on the order 10^{-3} Ohm.cm^2) are higher than the state-of-the-art ones known from literature (on the order $10^{-5} - 10^{-6}$ Ohm.cm^2) [16], both types of contacts yield good electrical performance and ohmic behavior. Despite the observed granular structure and strong metal intermixing in the Ti-based stacks, these multilayered structures show electrical performance as good as the Ta-based ones. A key point for the good performance could be the formation of appropriate conductive titanium or tantalum nitride layers at the interface with GaN ensuring very low Schottky barrier. Although the nitride layer is experimentally found only for the Ti case, we can assume formation of a tantalum nitride film also in the Ta-based stacks because the specific contact resistance value is the same for the both types of metallization.

4 Conclusions

Structure, composition, mechanical and electrical properties of Ti/Al/Ti/Au and Ta/Al/Ta metal stacks fabricated by e-beam evaporation and thermal annealing on n-type GaN films are studied.

Strong intermixture of metal components used for the Ti-based stacks is observed. In particular, Au from the top layer is found to diffuse downwards to the GaN interface, while Ga diffuses upwards intermixing with Au. Ti of the bottom layer diffuses into GaN forming a layer of titanium nitride. Layers of the Ta-based stacks have smoother interfaces compared to the Ti-based ones. The top Ta and intermediate Al layers are continuous. The bottom Ta layer shows granular structure most probably due to strong lattice mismatch with GaN and possibly due to partial diffusion followed by tantalum nitride formation. Our data on smooth interfaces and morphology for Ta-based stacks as well as on the granulation of Ti-based ones are in good correlation with earlier publications, alongside providing detailed insights into composition evolution of the ohmic contacts.

Results of the four-point bending tests show that the cracks always develop at the interfaces between Si and buffer layers of GaN film but the fabricated metal stacks never become exfoliated. This is an evidence for

good adhesion of both the Ti- and Ta-based metal contacts to GaN, which would ensure high reliability of the electrical connections.

Measurements of current-voltage dependences show ohmic behavior with the same specific contact resistance, ca. 1.2×10^{-3} Ohm.cm^2, for the both types of stacks despite lower structural and compositional perfectness of the Ti-based structures compared to the Ta-based ones. This might lead us to an assumption that formation of high-conductive metal nitrides at GaN interface is one of the key issues for making ohmic contacts, while the structure of upper metal layers is important mostly in terms of further contact optimization, for instance, for wire bonding or in terms of a long-term stability.

References

1. J. Millan, P. Godignon, X. Perpina, A. Perez-Tomas, J. Rebollo, IEEE Transact. Power Electron. **29**(5), 2155-2163 (2014).

2. E.A. Jones, F. Wang, D. Costinett, IEEE J. Emerg. Select. Topics Power Electron. **4**(3), 707-719 (2016).

3. H. Amano et al. J. Phys. D: Appl. Phys. **51**, 163001 (2018).

4. D. Shahin, A. Christoua, ECS Transactions **64(7)**, 203–211 (2014).

5. H. Jin, L. Qin, L. Zhang, X. Zeng, R. Yang, MATEC Web Conf. **40**, 01006 (2016).

6. V.N. Bessolov, E.V. Konenkova, S.A. Kukushkin, A.V. Osipov, S.N. Rodin, Rev. Adv. Mater. Sci. **38**, 75-93 (2014).

7. S.A. Kukushkin, A.V. Osipov, V.N. Bessolov, B.K. Medvedev, V.K. Nevolin, K.A. Tcarik, Rev. Adv.

Mater. Sci. **17**, 1-32 (2008).

8. M.M. Rozhavskaya, S.A. Kukushkin, A.V. Osipov, A.V. Myasoedov, S.I. Troshkov, L.M. Sorokin, R.S. Telyatnik, R.R. Juluri, K. Pedersen, V.N. Popok, Phys. Stat. Sol. A **214**(10), 1700190 (2017).

9. V.N. Popok, T.S. Aunsborg, R.H. Godiksen, P.K. Kristensen, R.R. Juluri, P. Caban, K. Pedersen, Rev. Adv. Mater. Sci. **57**(1), 72-81 (2018).

10. O. Ambacher, J. Smart, J.R. Shealy, N.G. Weimann, K. Chu, M. Murphy, W. J. Schaff, L. F. Eastman, R. Dimitrov, L. Wittmer, M. Stutzmann, W. Rieger, J. Hilsenbeck, J. Appl. Phys. **85**(6), 3222-3233 (1999).

11. E. Ahmadi, S. Keller, U.K. Mishra, J. Appl. Phys. **120**, 115302 (2016).

12. J. Bergsten, J.-T. Chen, S. Gustafsson, A. Malmros, U. Forsberg, M. Thorsell, E. Janzen, N. Rorsman, IEEE Transact. Electron. Dev. **63**(1), 333-338 (2016).

13. V. Portz, M. Schnedler, H. Eisele, R. E. Dunin-Borkowski, Ph. Ebert, Phys. Rev. B **97**, 115433 (2018).

14. G. Greco, F. Iucolano, F. Roccaforte, Appl. Surf. Sci. **383**, 324-345 (2016).

15. A. Motayed, R. Bathe, M.c. Wood, O.S. Diouf, R.D. Vispute, S. Noor Mohammad, J. Appl. Phys. **93**, 1087 (2003).

16. L. Pang, K. Kim, Mater. Sci. Semicond. Proces. **29**, 90-94 (2015).

17. A. Malmros, H. Blanck, and N. Rorsman, Semicond. Sci. Technol. **26**, 075006 (2011).

18. A. Pooth, J. Bergsten, N. Rorsman, H. Hirshy, R. Perks, P. Tasker, T. Martin, R.F. Webster, D. Cherns, M.J. Uren, M. Kuball, Microelectron. Reliabil. **68**, 2-4 (2017).

19. I. Hofinger, M. Oechsner, H.-A. Bahr, and M.V. Swain, J. Fracture **92**, 213-220 (1998).

20. B.P. Johnson, and C.I. Huang, J. Electrochem. Soc. **125**(3), 473-475 (1978).

21. G. K. Reeves, Sol.-State Electron. **23**, 5, 487-490 (1980).

22. L. Wang, F.M. Mohammed, I. Adesida, J. Appl. Phys. **103**, 093516 (2008).

23. A. Fontserè, A. Pérez-Tomás, M. Placidi, J. Llobet, N. Baron, S. Chenot, Y. Cordier, J. C. Moreno, P. M. Gammon, M. R. Jennings, M. Porti, A. Bayerl, M. Lanza, M. Nafría, Appl. Phys. Lett. **99**(21), 213504 (2011).
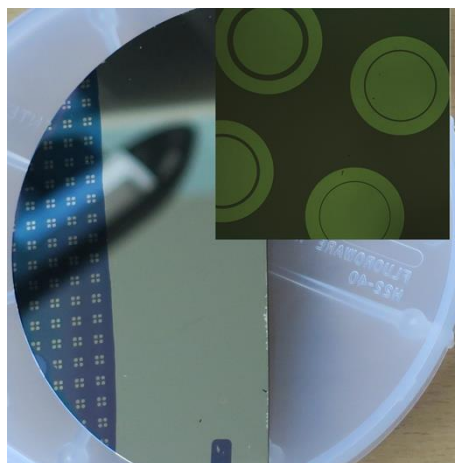
Fig. 1. Photo of a half-wafer with ring-shaped contacts (left) and continuous films (right). Insert represents 10x-magnified optical microscope image showing the contact structures.
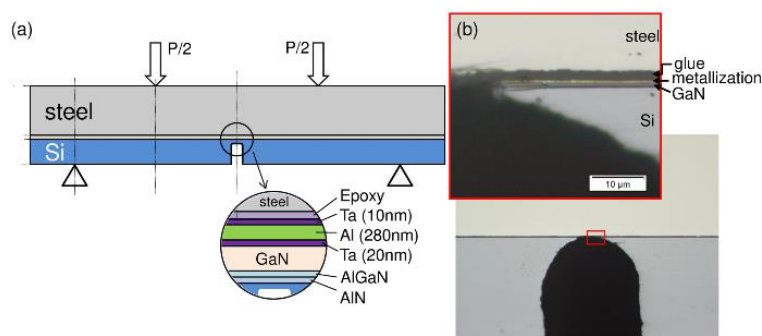

Fig. 2. (a) Schematic picture of a sandwich type sample structure prepared for 4PB tests exemplary for the Ta-based stack. (b) Optical microscope images with different magnification of a sample prior to testing.
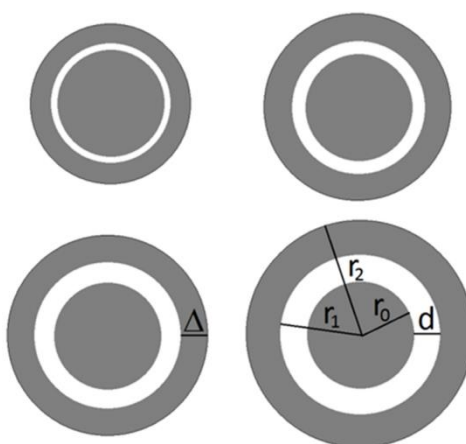

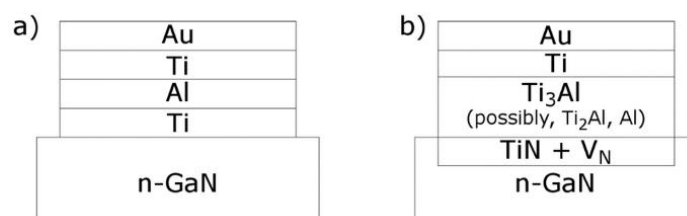Fig. 3. Geometry of metal contacts. See text for explanation of notations.

Fig. 4. Schematic pictures of (a) as-deposited Ti/Al/Ti/Au multilayered structure on n-type GaN and (b) the

expected formation of compounds after high-temperature sintering (prepared after the results of [15]).
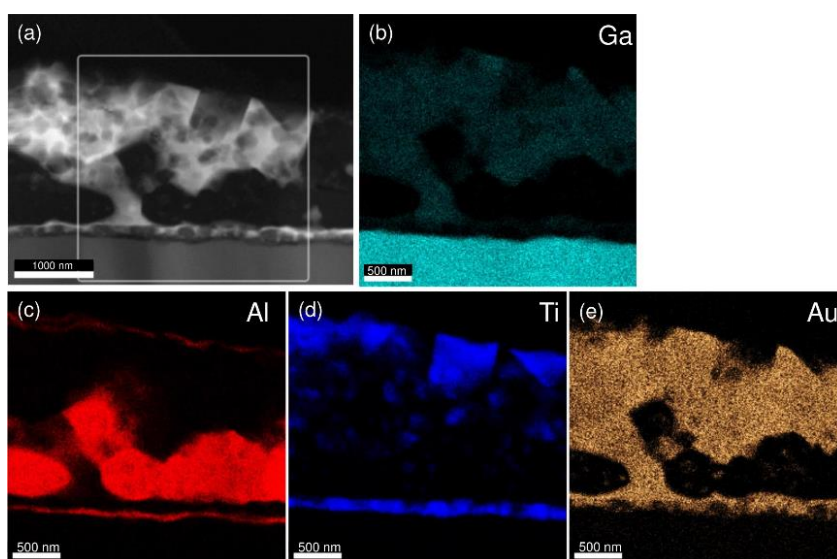
Fig. 5. (a) STEM HAADF image of the sintered Ti-based metal stack cross-section and (b-e) spatial maps

(obtained by EDX analysis) of different metals indicated in every panel for the marked area shown in (a).
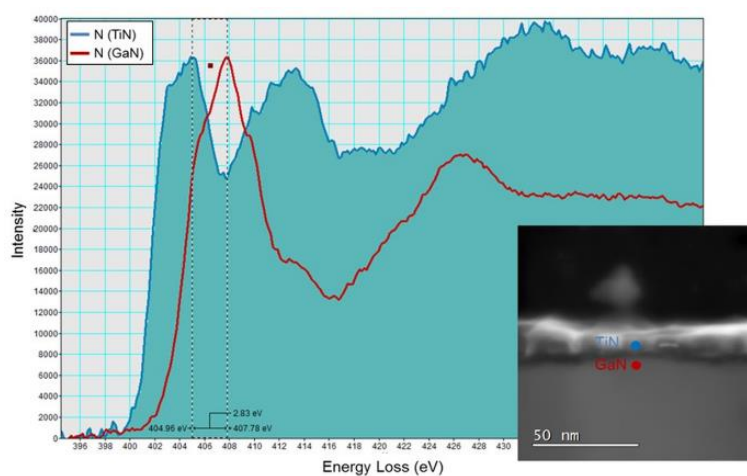

Fig. 6. EELS of N K-edge corresponding to GaN and TiN, thus, revealing titanium nitride formation at the

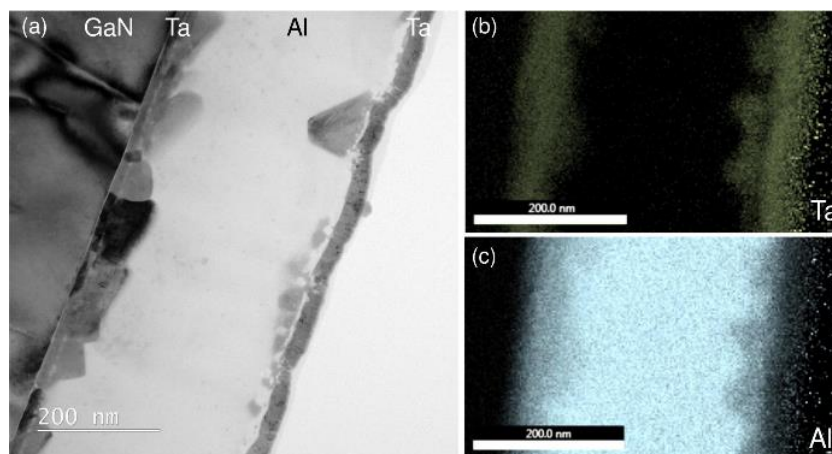metal stack/GaN interface, which is shown by STEM image in the insert.

Fig. 7. (a) TEM image and elemental maps for (b) Ta and (c) Al obtained by EDX on the Ta-based stack cross-section.
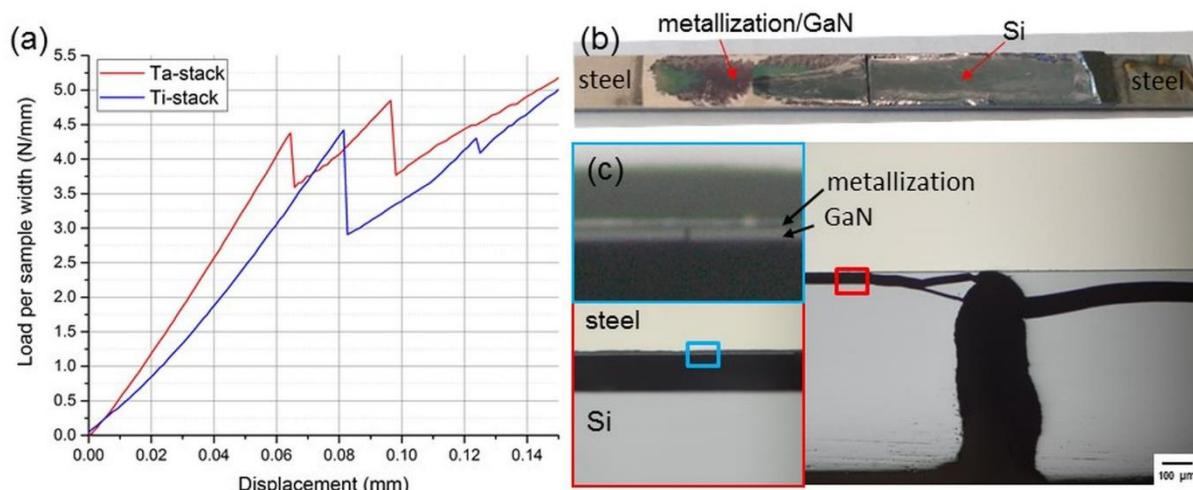

Fig. 8. (a) Representative load-displacement curves of the 4PB test for both metallization film stacks. (b) Fully separated fracture surface adhered to the steel stiffener and (c) cross sectional optical microscope images of a tested Ta-sample with increasing magnification from right to bottom-left and then top-left.
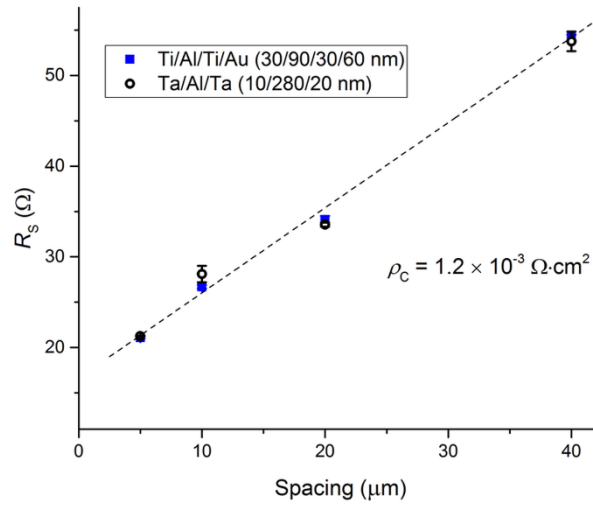
Fig. 9. Series resistance as a function of spacing between the central circle and surrounding rings in CTLM measurements for Ti- and Ta-based stacks. Both cases can be fitted with same dashed line yielding contact resistivity indicated in the plot.
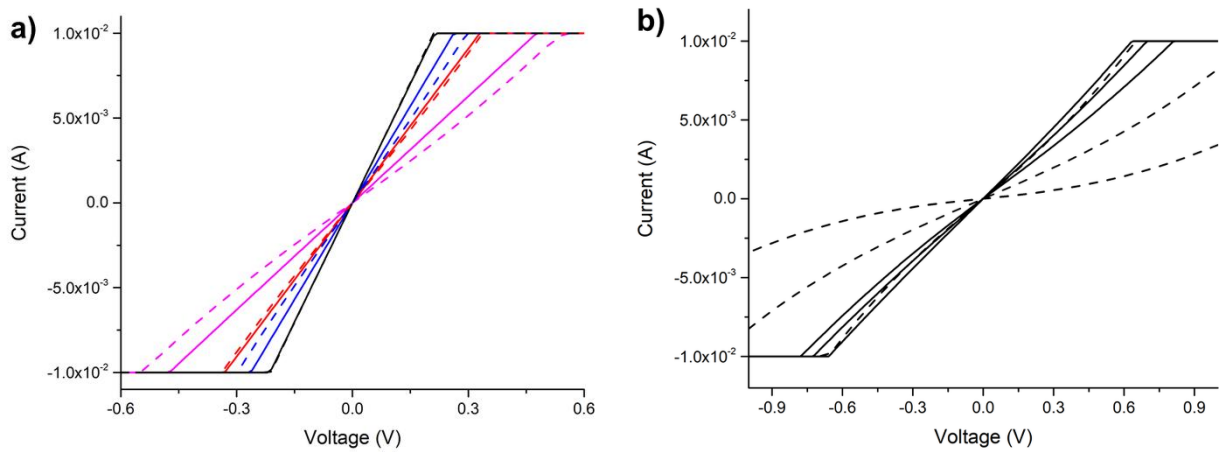

Fig. 10. Current-voltage dependencies of Ta- (dashed lines) and Ti-based (solid lines) stacks (a) showing linear character for the contacts spaced by 5 (black), 10 (blue), 20 (red) and 40 (pink) µm and (b) showing quasi-linear character for some selected 40 µm-spaced Ta- (dashed lines) and Ti-based (solid lines) stacks.